STRUCTURE OF SPACEBORNE LIDAR RETURNS FROM THE CLOUD TOP. PART I. OPTICALLY HOMOGENEOUS CLOUDS

G.M. Krekov and M.M. Krekova

State Medical University, Tomsk
Institute of Atmospheric Optics,
Siberian Branch of the Russian Academy of Sciences, Tomsk

Received June 6, 1997

We present here estimates of return signals of an orbiting lidar intended for sounding clouds. The estimates are obtained using Monte Carlo method. The calculations are performed for $\lambda = 0.532$ μm. *Here we analyze the clouds of a homogeneous optical structure. The signal structure is shown to vary within a cloud layer of* $\Delta H = 100$ m *depending on optical and geometrical conditions of the experiment. As follows from the analysis of the results extinction coefficient is the main parameter that determines the lidar return structure. Variations of the scattering properties of a cloud do influence the return signal formation only insignificantly.*

INTRODUCTION

The use of airborne lidar systems has shown their high efficiency when solving certain ecological and geophysical problems, studying the atmosphere and underlying surface, and so on. Use of lidars onboard satellites makes it possible to perform global measurements of the parameters which could be useful when solving certain problems. The prospects of using spaceborne lidars to study the atmosphere were formulated earlier[1] by the NASA working group. They consider among the basic measurements, those which are informative in monitoring of the distribution and total content of aerosol in the atmosphere as well as measurements of parameters of individual clouds and cloud fields.

The first measurement sessions have already been performed with the Russian lidar BALKAN at the MIR station[2] and the LITE lidar of NASA.[3] It is obvious that the first experiments are mostly tests (development of the measurement technique, classification of signals necessary for automation of the data processing). Interpretation of signals is more difficult due to inevitable interference of high background of different origin.

Some problems of lidar sounding of cloudiness can be revealed from the analysis of range finder signals which were used in space many times.[4] The authors of Ref. 5 have made an attempt to interpret range finder signals from the cloud. First of all the technique was developed for reconstructing the signal using threshold energy values. Several approaches to inverting such signals have been proposed recently. The values of the volume extinction coefficients obtained are quite in a wide range $\sigma_{\text{ext}} \approx 14\text{–}500\ \text{km}^{-1}$, that, in our opinion, can be related not only to the approximate reconstruction of the signals, but also to high level of multiple scattering.

In this paper we present some results of calculating the spaceborne-lidar returns carried out by the Monte Carlo method. As known, this method makes it possible obtaining estimates of the signals with the separation of the interaction multiplicities and the arrival angles of photons on the detector. It gives the basis for detailed analysis of the lidar return structure depending on the optical and geometrical conditions of the experiment. As a result, one can obtain information on sensitivity of the returns to variations in the parameters of both optical state of the medium and the experimental conditions.

The lidar return $P(h)$ from the scattering medium is the function of time or distance to the object under investigation. Normally, the single scattering signal $P_1(h)$ in the direction toward optical detector is considered as the principal carrier of information. In this case the received signal is described by known laser radar equation. In principle, measuring the signal amplitude and inverting the lidar equation, one can obtain the information on the optical state of the medium under investigation. The problem is complicated by the presence of the background noise of active origin, i.e. the interference created by the lidar return itself. It is caused by the phenomena of the secondary scattering of the photons within the limits of the angular aperture of the receiving device.

In recent years much attention has been paid to peculiarities in the formation of the background component of the signal. For example, Refs. 6–8 present some results of both statistical and analytical methods for calculating the return signal for the ground based, airborne, and spaceborne lidars. The papers add each other, because, normally only, one of the parameters of the problem is varied in them.

In this paper we present the results of modeling the spaceborne lidar return from the upper boundary of clouds, obtained under specific initial and boundary conditions. The analysis has shown that in many cases the results obtained with a spaceborne lidar may be quite general.

STATEMENT OF THE PROBLEM

The radiation transfer equation was solved by the Monte Carlo method for the initial and boundary conditions characteristic of a monostatic laser radar. Let the lidar be $H_0 = 400$ km far from the Earth's surface. Let the source emit isotropically within the cone $2\pi\,(1 - \cos\varphi_i)$, where $\varphi_i = 0.2$ mrad is the divergence angle of the source. The return signal is recorded with a detector in the angular cone $2\pi\,(1 - \cos\varphi_d)$, where $\varphi_d = 0.4$ mrad is the angular aperture of the detector. Calculations were made for the rectangular pulse of the duration $\tau_i = 10$ nsec and energy $W_0 = 1$ J. The transmission coefficient of the transmitting-receiving system was taken to be $k_p = 1$. The optical properties of the scattering media were set by the extinction coefficient $\sigma_{ext}(h)$, single scattering albedo $\Lambda(h)$, and the scattering phase function $g(\vartheta)$, where ϑ is the scattering angle. The cloud layer is at the altitude range 1.5 to 2 km above the Earth's surface had the scattering properties corresponding to the C1 and C2 types of the classification from Ref. 9. We considered stratus clouds without breaks. The aerosol extinction in the 30 km layer of the atmosphere above the clouds was taken into account. The altitude model of $\sigma_{ext}(h)$ and $\Lambda(h)$ of the atmospheric aerosol were set according to the background model,[10] and its scattering phase function corresponded to haze H.[9] The calculations were made for a lidar operating at the wavelength $\lambda = 0.532$ μm with the representative statistical volume of 5 to 10 million photon events in every calculation. The volume of the statistical sample was increased as the optical density of the medium decreased. It should be noted that the calculations were made for the upper boundary of the cloud layer of the thickness $\Delta H = 100$ m. The dependences of different functionals on the value h equivalent to the accumulated path or time t of the photon staying in the medium, i.e. $h = ct/2$, where c is the light velocity, are shown in the figures. The functional histograms are constructed using the strobe intervals $\Delta h \le c\tau_i$, i.e. they do not exceed the spatial length of the pulse.

RESULTS OF CALCULATIONS

Calculation of the power $P(h)$ of the lidar returns from homogeneous C1 clouds of different optical thickness is presented in Fig. 1. Significant difference in the absolute levels of amplitudes $P(h)$ are observed up to about 20 m depth into the cloud. The rate of the amplitude variation in this region depends on the value σ_{ext} and increases with its increase. The qualitative transformation of the $P(h)$ behavior occurs at the depth of 20 to 40 m. The absolute levels of signals approach each other, the signal from a more dense medium has lower value. The results presented in Fig. 1 show that situations may occur in this area when the signals $P(h)$ of the same power come to the detector from clouds with different values σ_{ext}. Such an amplitude-temporal behavior of the signal may be explained as follows. The number of multiple interaction orders taking part in the formation of signal from a cloud layer of thickness $\Delta H \approx 100$ m at low extinction coefficient values $\sigma_{ext} \le 20$ km^{-1} is not high, but their contributions are high due to the lower extinction of radiation in the medium. The number of multiple interaction order increases at increasing values σ_{ext}, but their contributions decrease. Therefore the resulting signals are almost the same in both cases. It should be noted, however, that at $\sigma_{ext} \ge 70$ km^{-1} there no compensation occurs and a more sharp decrease of the pulse is observed. At the values $\sigma_{ext} = 70$ and 100 km^{-1} this occurs at the depth of 80 and 60 m, respectively. Analysis of the results presented in Fig. 1 allows one to note the following. The choice of a portion within the pulse is important for the reconstruction of the medium optical parameters. To obtain information on the optical properties of a homogeneous cloud it is more expedient to use the front edge of the pulse, because the use of the part of the signal coming from the depth of 20 to 40 m can lead to ambiguous results of the inversion.

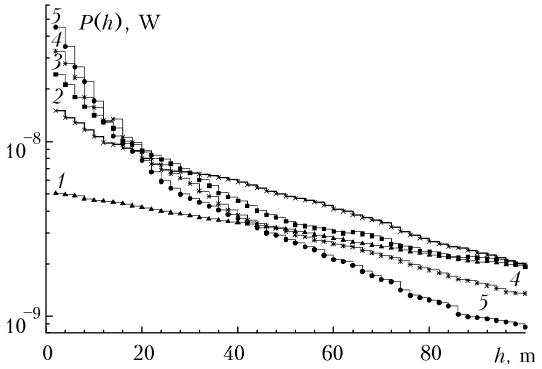

FIG. 1. The return signal power $P(h)$ as a function of the depth into the cloud. Curves 1–5 are calculated for the values $\sigma_{ext} = 10$, 30, 50, 70, and 100 km^{-1}, respectively.

The calculations similar to those presented in Fig. 1 were also performed for the scattering phase function characteristic of a C2-type cloud. The results do not deserve illustration, because they are practically the same. The dependence of signal power $P(h)$ on the angular size of the detector is also weak. Neither the increase of the detection angle by one order of magnitude, i.e. up to the value $\varphi_d = 4.4$ mrad, nor the decrease to the value $\varphi_d = \varphi_i$ do lead to a significant variation of $P(h)$. The weak dependence on the angular size of the detector is obviously related to big size of scattering volumes within the viewing cone, since the cross size of the beam at the upper boundary of the cloud is comparable with the cloud layer thickness. As a consequence, the radiation scattered in the side directions does not escape the viewing cone and takes part in the subsequent formation of the diffuse scattering flux.

Much more essential variations of the signal $P(h)$ occur at a significant decrease of the sounding beam divergence. Narrowing of the angle φ_i down to the value $\varphi_i = 0.01$ mrad and $\varphi_d = \varphi_i$ leads to a more sharp decrease of the trailing edge of the pulse. It is illustrated by the results of calculations presented in Fig. 2 for two divergence angles of the sounding beam and two values of the extinction coefficient σ_{ext}.

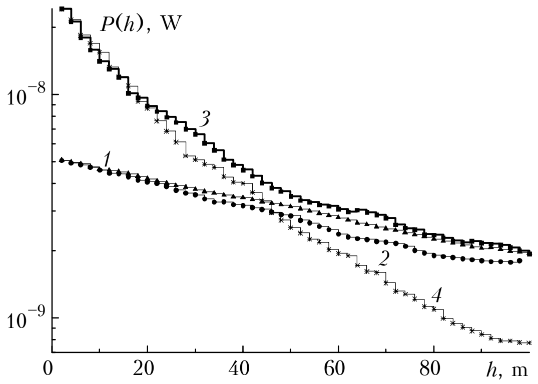

FIG. 2. The change of $P(h)$ depending on the angular size of the transmitter and detector apertures. The curves 1, 3 and 2, 4 are calculated for $\varphi_i = 0.2$ *and* 0.02 mrad, *respectively; 1, 2 and 3, 4 correspond to the values* $\sigma_{ext} = 10$ *and* 50 km^{-1}, *and* $\varphi_d = \varphi_i$.

The absolute level of the signal $P(h)$ from the leading edge of the pulse formed by the radiation of low orders of scattering does not depend on the value φ_i and is determined only by the optical density of the medium. The sharp decrease of the signal from the trailing edge of the pulse is observed for clouds with high optical density due to a decrease of contributions from higher orders of scattering. The distribution of the reflected radiation over the multiple interaction orders is shown in Fig. 3*a* for the aforementioned value $\varphi_d = 0.44$ mrad.

The calculation was performed for a cloud with the extinction coefficient $\sigma_{ext} = 50$ km^{-1}. The figures at the curves *1–5* correspond to the order of multiple scattering $P_i(h)$, and *6* is the total signal $P(h)$. The dominating role of the first scattering order is observed up to $\tau \approx 0.8$, then the absolute value of signals from the higher orders successively increases, and their contribution into the total signal becomes comparable at $\tau \approx 1.2–2.5$. Most decisive redistribution among the contributions from multiple scattering orders occurs at the depth $\tau \geq 2$, i.e. higher orders of scattering begin to prevail and make the determining contribution into the total signal. Figure 3*b* shows the percentage of the signals from the first order scattering into the total signal $K_1(h) = P_1(h)/P(h)$, the curve is marked by the symbol Σ_1, then the sum of contributions from two first orders is $K_2(h) = (P_1(h) + P_2(h))/P(h)$, and so on.

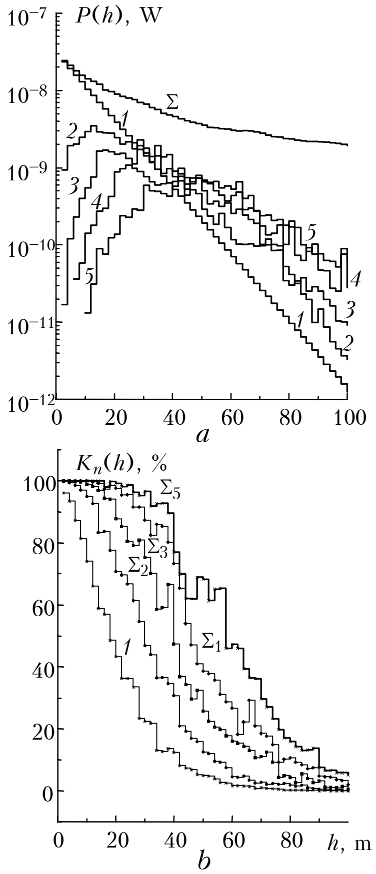

FIG. 3. Redistribution of the reflected radiation $P(h)$ over orders of multiple scattering (a) and the percentage $K_n(h)$ of the contributions of the first order, the sum of the first and second orders and etc. into the total signal (b). The cloud scattering coefficient is $\sigma_{ext} = 50$ km^{-1}.

The single scattering signal is no less than 50% of the total signal power up to $\tau \approx 1$. The account for the second order scattering increases this optical depth up to $\tau \approx 1.5$. Only the sum of five orders makes it possible to take into account the greatest portion of the power of radiation coming to the detector from the depth $\tau \approx 2.5–3$. The total fraction of the multiple scattering background in the return signal is illustrated by the results shown in Fig. 4. It shows the ratio of the power of the background component to the total signal calculated for the clouds with different optical density. The background component due to multiple scattering in a cloud with the extinction coefficient of $\sigma_{ext} \leq 10$ km^{-1} does not play a determining role in the total signal $P(h)$ for all depths up to $\Delta H = 100$ m. The multiple scattering background at $\sigma_{ext} \geq 50$ km^{-1} becomes the main part of the signal starting from the depth of 10 to 20 m from the upper boundary of the cloud.

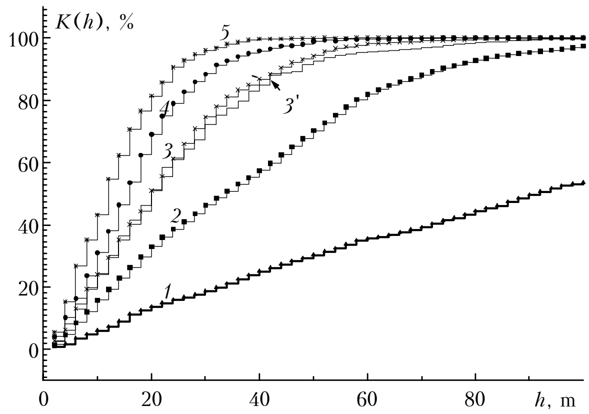

FIG. 4. Percentage of the multiple scattering background in the reflected signal as a function of the depth of the layer sounded. Curves 1–5 are calculated for the values σ_{ext} = 10, 30, 50, 70, *and* 100 km^{-1}; *3′ is the calculation for* φ_{i} = 0.02 *and* σ_{ext} = 50 km^{-1}.

The results presented above can serve as a basis for selection of the methods for processing the return signals from the clouds. They make it possible to determine the admissible limits of applicability of the radar equation written both in the single scattering approximation and taking into account the higher orders of scattering. They allow one to make a decision on selection of the multiple scattering background which is possible until the single scattering fraction makes the noticeable part of the total signal. In addition, they show the expedience of using the background component of the signal, at some portions of the pulse, as a carrier of useful information.

CONCLUSION

Reliable recording the cloud formations of different optical density depends on the sensitivity available in the measurement channel of the lidar. The data presented in Fig. 5 illustrate the dependence of the maximum signal power on the optical density of clouds. It is linear and is described by the simple regression relationship

$$P_{\text{max}} = A + B\ \sigma_{\text{ext}}\ [\text{km}^{-1}],$$

where $A = 0.18{\cdot}10^{-8}$ and $b = 0.43{\cdot}10^{-9}$.

This relationship allows one to estimate the power of radiation reflected from the upper boundary of clouds with the extinction coefficients in the range from 1 to 100 km^{-1}. It is quite universal due to only weak dependence of the scattering power from the leading edge of the pulse on both geometrical parameters of the transmitting-receiving system and on the scattering phase function of the cloud. The estimate can easily be refined for lidars with the parameters different from the calculated ones in the orbit altitude or in the initial power of the pulse. To do this, the values P_{max} shown in Fig. 5 should be multiplied by corresponding coefficients $K_H = H^2/(H \pm \Delta H)^2$ and $K_W = (W \pm \Delta W)/W$, where H = 400 km and W = 1 J, as it was mentioned at the beginning of the paper.

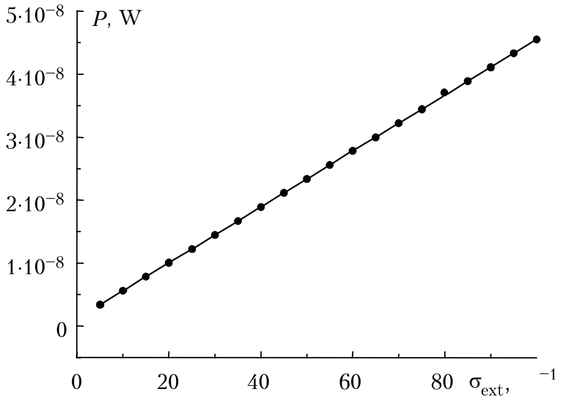

FIG. 5. Change of the maximum power of radiation reflected from the upper boundary of a cloud layer $\Delta h = c\tau_{\text{i}}$ *as a function of the cloud optical density.*

REFERENCES

1. V.J. Abreau, Optical Engineering **19**, 489–493 (1980).

2. Yu.S. Balin, A.A. Tikhomirov, and S.S. Samoilova, Atmos. Oceanic Optics **10**, No. 3, 209–220 (1997).

3. R.H. Couch, C.W. Rowland, K.S. Ellis, et al., Optical Engineering **30**, 88–95 (1991).

4. J.L. Buffton, Proc. IEEE **77**, No. 3, 71–88

5. G.P. Kokhanenko, G.G. Matvienko, V.S. Shamanaev et al., Atmos. Oceanic Optics **7**, No. 7, 517–521 (1994).

6. L.R. Bissonette and D.L. Hutt, in: *Proceedings of the Fourth International Workshop on Multiple Scattering Lidar Experiments* (Italy, 1990), pp. 10–21.

7. Y.Okasaki, K. Noguchi, H. Okumura, and N. Takeuchi, *Abstracts of Papers of the 17th International Laser Radar Conference*, Sendai (1994), pp. 131–133.

8. E.P. Zege, I.L. Kotaev, L.N. Polonskii and A.A. Kokhanovskii, in: *Abstracts of Papers of the 17th International Laser Radar Conference*, Sendai (1994), pp. 133–134.

9. D. Deirmendjian, *Electromagnetic Scattering on Spherical Polydispersions* (Elsevier, New York, 1969).

10. V.E. Zuev and G.M. Krekov, *Optical Models of the Atmosphere* (Gidrometeoizdat, Leningrad, 1986), 255 pp.